ATMOSPHERIC EXCITATION OF THE CHANDLER WOBBLE ALONG THE 20TH CENTURY: INSIGHTS FROM ECMWF ERA-20C REANALYSIS

S. LAMBERT

Observatoire de Paris, Université PSL, CNRS - France - sebastien.lambert@obspm.fr

ABSTRACT. We used the grids of the ECMWF ERA-20C atmospheric global circulation model to compute the atmospheric excitation and torques in the Chandler frequency band over 1900-2010. We showed that (i) the atmosphere acts dominantly over Eurasia (via a mountain torque on the Tibetan plateau and a large variability of the angular momentum over Western Siberia) with strong bursts in the AAM around 1910, 1940 and the 1970s, and (ii) the mountain torque appears to be correlated with North Atlantic modes (AMO, NAO, AO). The study suggests that the variability of the Chandler wobble at decadal/multidecadal time scales is controlled by the North Atlantic/Arctic system that acts mainly on the Tibetan mountains.

1. INTRODUCTION

The Earth's Chandler wobble is a free rotational mode of the mantle associated with the Earth's ellipticity whose period is close to fourteen months in the rotating frame and amplitude is about 0.2 arcsecond, strongly variable. Its excitation mechanism has remained quite mysterious long after its discovery at the end of the 19th century, until the development of atmospheric and oceanic circulation models shed new lights. It is now admitted that the Chandler wobble is fueled through continuous atmospheric and oceanic mass redistribution (Gross 2000; Brzeziński and Nastula 2002; Bizouard et al. 2011). Most of the studies rely on the recent period covered by the standard global circulation reanalyses released by the main climate center like the National Center for Environmental Prediction/National Center for Atmospheric Research (NCEP/NCAR) or the European Center for Medium-range Weather Forecast (ECMWF). However, the recent development of century reanalyses, at least for the atmosphere, opens new perspectives on assessing the excitation of the Chandler wobble, measured since 1860, by the Earth's external fluid layers.

This work uses the ECMWF ERA-20C reanalysis data to assess the atmospheric contribution to the Chandler wobble over the entire 20th century. Although we miss the oceanic contribution, we nevertheless reveal the regional interactions between the atmosphere and the solid Earth as well as possible impact of global climate oscillations.

2. DATA AND METHODS

We used grids of surface pressure, instantaneous north/eastward turbulent stress, zonal and meridional wind speeds at 17 pressure levels between 10 and 1000 mBar as provided by the ECMWF ERA-20C reanalysis (Poli et al. 2015) covering 1900-2010. Gridded values are directly monthly means of 6-hourly model output. The spatial resolution was set to $2^\circ \times 2^\circ$. From local values of the variables, we obtained local values of the pressure and wind terms of the atmospheric angular momentum (AAM) as well as mountain and friction torques following standard formulations (Barnes et al. 1983; Huang et al. 1999). The mountain torque was computed using the orography of the model. Then, to obtain the AAM and torques contained only in the Chandler frequency band, we filtered AAM and torques in time domain by applying a Panteleev filter (Panteleev and Chesnokova

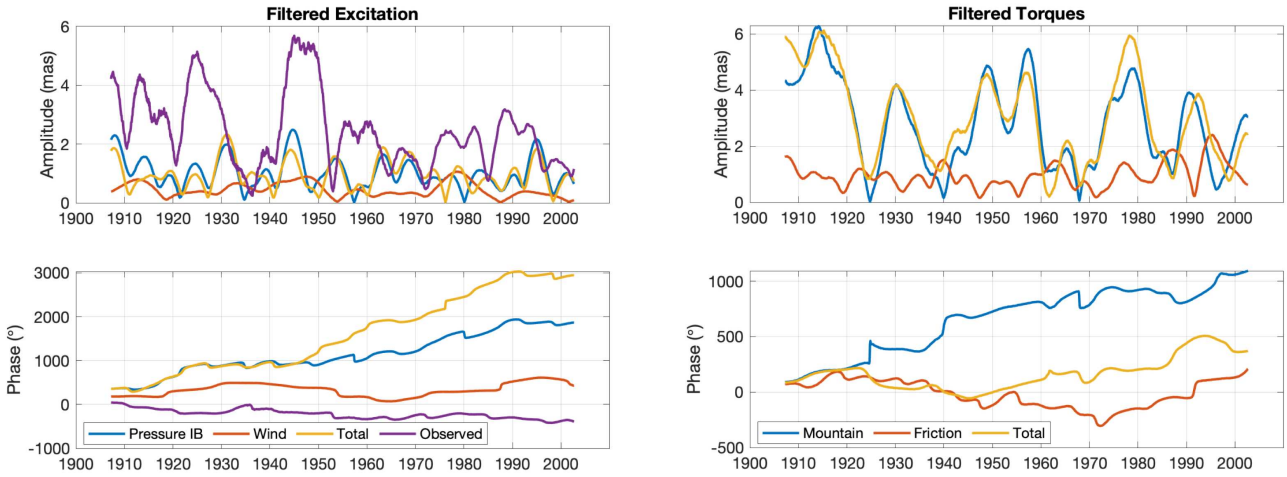

Figure 1: Amplitudes and phases of the complex excitation and torques in the Chandler frequency band.

2011) of bandwidth 35 days and central period 430.3 days. We removed 7 years of data at the beginning and the end of the filtered series in order to account for edge filtering effects, thus letting an effective period covering 1907-2003. The choice of the central frequency and the bandwidth is debatable: we rely on previous studies using similar values (e.g., Zotov and Bizouard 2012; 2015) and on the fact that the window should not be too large to avoid catching the premises of the annual wobble.

The observed excitation was derived from the observed polar motion series taken at the International Earth rotation and Reference systems Service (IERS) EOP C01 provided by the IERS Earth Orientation Center (Bizouard et al. 2019). The excitation was derived following Wilson (1985) and then filtered to keep only the signal in the Chandler frequency band.

Regarding climate indices, we searched for long datasets, resulting is some inhomogeneity since the different series were generally based on different datasets. We retrieved the Atlantic Multidecadal Oscillation (AMO) index from the Earth System Research Laboratory (ESRL) of the National Oceanic and Atmospheric Administration (NOAA). It is derived from the Kaplan extended sea surface temperature (SST) data set (Kaplan et al. 1998) and starts in 1856. The Pacific Decadal Oscillation (PDO) was derived from the UKMO Historical SST data set for 1900-81 and made available by the Joint Institute for the Study of Atmosphere and Ocean (JISAO), University of Washington. We also considered the Southern Oscillation Index (SOI), the North Atlantic Oscillation (NAO), the Arctic Oscillation (AO), and the Antarctic Oscillation (AAO), all derived from the NOAA 20C reanalysis (Compo et al. 2011).

All time series were made consistent by resampling geodetic data and climate indices at the epochs of the final AAM and torque series.

3. DISCUSSION AND CONCLUSION

The filtered time domain globally integrated quantities are shown in Figure 1. The atmospheric excitation is dominated by the surface pressure with prominent activity in 1930, 1940, and 1995. It is far insufficient to explain the observed geodetic excitation that shows large peaks in 1925 and 1945, letting a possible important contribution from the oceans but also for a deficiency of the current atmosphere reanalysis. The mountain torques strongly dominates the total torque.

The Figure 2 represents the regression of the local excitation and torques onto their globally integrated values (allowing to locate the regions that are the most representative of the global

activity) and the Hovmoeller (time-latitude and time-longitude) diagrams (that allow to get a time-domain view of the activity). The charts reveal the existence of 'hot spots' concentrating the interaction between the atmosphere and the solid Earth. The surface pressure excitation is thus dominated by Eurasia, consistently with a mountain torque essentially acting over the Himalaya and the Tibetan plateau, fueled by meridional pressure gradients between Siberia and Southern Eurasia. Strong bursts in this Eurasian excitation are observed circa 1910, 1940, and 1970. A relatively important mountain torque is seen around the Antarctic plateau with an interannual variability. Note that a strong mountain torque does not necessarily correspond to a high AAM, the latter being the time integration of the former, a persistently (even moderately) high mountain torque is relevant to lead to a high AAM. The wind AAM and friction torque pictures are consistent with what one can expect from pressure patterns (e.g., strong surface wind and friction torque acting at the west entry of the surface pressure pattern, i.e., over Western Europe) and are not shown here.

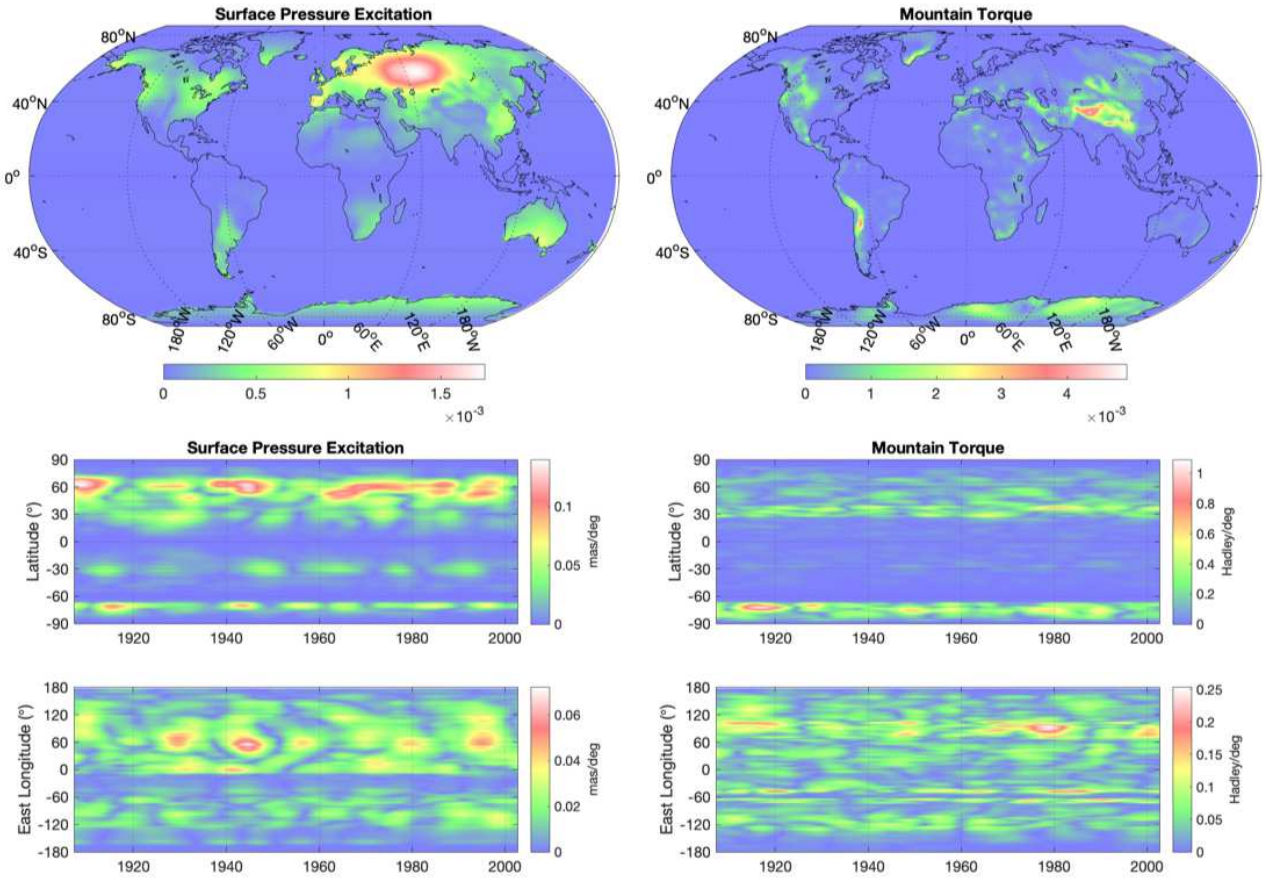

Figure 2: (Top) Regression of the local pressure AAM and mountain torque onto the global pressure AAM and mountain torque. (Bottom) Time-latitude and time-longitude (Hovmoeller) diagrams of the surface pressure excitation and mountain torque.

The activity of the surface pressure and mountain torque being strongly localized, one could ask whether their time variations are connected to local climate modes like, e.g., the various climate modes inherent to the North-Atlantic/Eurasia system (NAO, AO, AMO). To test this hypothesis, we computed the Pearson correlation coefficients r between various climate indices with global surface pressure excitation and the mountain torque for several time lags (Table 1). One has

to note that short time lag (say less than 10 years) might be understood as 'no lag' since the Panteleev filtering acts as a smoothing window of about 7 years. The significance of the correlation was evaluated using the null hypothesis that detrended series are independent AR1 processes (e.g., Anderson 1958) under which the sample value of the Fisher z-transformation of the correlation is expected to differ from zero by a number $s = z\sqrt{\mathrm{DOF} - 3}$ of standard deviations. Here, DOF is the number of degrees of freedom and can be estimated as the ratio of the length of the series to the length of the segment corresponding to the decorrelation time (itself deduced as the lag for which the autocorrelation function decreases to $1/e$). We highlight below the correlations with small lags (here given in years) and Fisher s coefficient larger than 2, i.e., providing a probability of rejection of the null hypothesis larger than 95%. Thus, we detected a possible connection of the surface pressure excitation with the AAO and of the mountain torque with the NAO, the AO and the AMO. These results are consistent with the finding of a mountain torque detected on the edge of the Antarctic plateau and the surface pressure pattern found over Eurasia on the regression map varying at interannual and multidecadal time scales, producing a strong mountain torque on the Himalayan and Tibetan mountains. Note that the inconsistency between the climate indices (some of them being dependent on another circulation model) and ERA-20C grids may lead to miss some correlations or misestimate their statistical significance: ideally, the indices should be derived from the ERA-20C data.

		X			Y		
		r	Lag (yr)	s	r	Lag (yr)	s
Global Pressure Excitation	AAO	**0.599**	**0.2**	**3.0**	-0.365	-37.3	2.3
	AMO	-0.469	10.8	1.5	-0.380	9.4	1.1
	AO	-0.357	-15.4	1.7	-0.419	-25.3	2.0
	NAO	0.235	-13.3	1.2	**-0.387**	**2.3**	**2.0**
	PDO	0.489	26.8	2.2	0.415	17.9	1.5
	SOI	-0.320	26.6	1.7	-0.422	16.7	2.2
Global Mountain Torque	AAO	**-0.416**	**-4.3**	**2.0**	-0.448	15.9	2.4
	AMO	**0.760**	**0.0**	**2.5**	-0.420	15.8	1.2
	AO	**-0.593**	**9.2**	**3.3**	0.321	-37.2	1.3
	NAO	**-0.469**	**8.9**	**2.6**	**-0.541**	**7.5**	**3.1**
	PDO	-0.562	20.6	2.4	0.479	29.5	2.3
	SOI	-0.608	-19.5	4.2	-0.286	-24.4	1.3

Table 1: Pearson correlation coefficient r and optimal lag between the globally integrated surface pressure excitation and mountain torque and various climate indices. The coefficient s represents the Fisher z-score interpreted as a measurement of the significance of the correlation estimates.

In conclusion, our study suggests that the variability of the Chandler wobble at decadal and multidecadal time scales is controlled by the North Atlantic/Arctic system that produces surface pressure variations over Siberia and, as a consequence, a mountain torque on the Tibetan mountains. Although never done over such a long period, this study remains partial since (i) no ocean data were used and (ii) only one atmospheric circulation model was tested. It can be continued in two directions. The first one is completing the atmospheric study with ERA-20C ensemble members in order to evaluate a model error and introduce at least one other reanalysis, possibly from an independent meteorological center (e.g., the NOAA-CIRES-DOE Twentieth Century Reanalysis project; Compo et al. 2011). The second direction is to explore the recently released ocean reanalyses (e.g., SODA, Carton and Giese 2008; ORA 20C, de Boisseson and Alonso-Balmaseda 2016) to test the closure of the AAM budget over an entire century. The comparison of the most

consistent models with the observed polar motion excitation could lead to understanding the causes of the historical minimum of the Chandler wobble in the 1920s (Guinot 1978) and assess whether the current minimum (likely reached mid-2018) is due to the same reasons.

4. REFERENCES

Anderson, T. W., 1958, "An Introduction to Multivariate Statistical Analysis", Wiley.

Barnes, R. T. H., R. Hide, A. A. White, and C. A. Wilson, 1983, "Atmospheric angular momentum fluctuations, length-of-day changes and polar motion", Proceedings of the Royal Society of London Series A 387, pp. 31-73.

Bizouard, C., S. Lambert, C. Gattano, J.-Y. Richard, and O. Becker, 2019, "The IERS EOP 14C04 solution for Earth orientation parameters consistent with ITRF 2014", J. Geodesy 1, pp. 1–13.

Bizouard, C., F. Remus, S. Lambert, L. Seoane, and D. Gambis, 2011, "The Earth's variable Chandler wobble", Astronomy & Astrophysics, 526:A106. de Boisseson, E. and M. Alonso-Balmaseda, 2016, "An ensemble of 20th century ocean reanalyses for providing ocean initial conditions for CERA-20C coupled streams", Technical Report 24, ECMWF.

Brzeziński A., and J. Nastula, 2002, "Oceanic excitation of the Chandler wobble", Advances in Space Research, 30(2), pp. 195-200.

Carton, J. A. and B. S. Giese, 2008, "A reanalysis of ocean climate using simple ocean data assimilation (SODA)", Monthly Weather Review 136(8), pp. 2999–3017, 2019/12/05.

Compo, G. P., J. S. Whitaker, P. D. Sardeshmukh, et al., 2011, "The twentieth century reanalysis project", Quarterly Journal of the Royal Meteorological Society 137(654), pp. 1–28.

Gross, R. S., 2000, "The excitation of the Chandler wobble", Geophys. Res. Lett. 27, pp. 2329–2332.

Guinot, B., 1972, "The Chandlerian Wobble from 1900 to 1970, A&A 19, p. 207.

Huang, H.-P., P. D. Sardeshmukh, and K. M. Weickmann, 1999, "The balance of global angular momentum in a long-term atmospheric data set", J. Geophys. Res. 104, pp. 2031–2040

Kaplan, A., M. A. Cane, Y. Kushnir, A. C. Clement, M. B. Blumenthal, and B. Rajagopalan, 1998, "Analyses of global sea surface temperature", pp. 1856-1991. J. Geophys. Res. (Oceans) 103(C9), pp. 18567–18589.

Panteleev, V., and T. Chesnokova. 2011, "Deconvolution problem in inertial gravimetry", Moscow University Physics Bulletin 66(1), pp. 78–82.

Poli, P., H. Hersbach, P. Berrisford, et al., 2015, "ERA-20C deterministic", Technical Report 20, ECMWF, Shinfield Park, Reading.

Wilson, C. R., 1985, "Discrete polar motion equations", Geophysical Journal 80, pp. 551–554.

Zotov, L. and C. Bizouard, 2012, "On modulations of the Chandler wobble excitation", Journal of Geodynamics 62, pp. 30–34.

Zotov, L. and C. Bizouard., 2015, "Regional atmospheric influence on the Chandler wobble", Advances in Space Research 55(5), pp. 1300–1306.